cussed above, ranges from $\pm 11.0\%$ for Sm^{143m} to $\pm 12.8\%$ for Er^{167m}.

The described reactions are the predominant ones produced by short-time irradiation of the respective rare-earth elements. Since the gamma spectra are simple, they are thereby well suited for use in activation analyses. Several of these reactions are currently being utilized by the Bureau of Mines at the Reno Metallurgy Research Center for analyzing the respective rare-earth constituents in titanium alloys and other compounds.

PHYSICAL REVIEW VOLUME 139, NUMBER 6B 20 SEPTEMBER 1965

Muon Capture in $(p\mu d)^+$ Molecules*

I-T. WANG,† E. W. ANDERSON,‡ E. J. BLESER,‡ L. M. LEDERMAN, S. L. MEYER,§
J. L. ROSEN,‖ AND J. E. ROTHBERG¶
Columbia University, New York, New York

(Received 5 April 1965)

The $(p\mu d)^+$ molecules and μ-He^3 atoms formed in liquid hydrogen were used to detect neutrons from muon capture by deuterons and from muon capture by He^3. In the experiment, a purified muon beam was stopped in a target containing ultra-pure liquid hydrogen with 0.32% deuterium added. Neutron–gamma-ray discriminating detectors and oscilloscope photography enabled us to measure the time distribution of neutrons from the following rare muon-capture processes:

$$\mu^- + d \rightarrow \nu + 2n,$$
$$\mu^- + He^3 \rightarrow \nu + n + d$$
$$\rightarrow \nu + 2n + p.$$

Knowledge of the time distributions of the various $(p\mu d)^+$ hyperfine states and of the μ-He^3 atoms was used to unravel the various muon-capture rates of interest. Converted to the μd atom case, the measured rate gives 365 ± 96 sec^{-1} for muon capture from the doublet state of μd. This is to be compared with the theoretical rate of 334 sec^{-1} predicted by the current phenomenological muon-capture theory; and it provides the simplest verification of the Pauli exclusion-principle effect in muon capture. The neutron rate from muon capture by He^3 was determined to be $(1.20 \pm 0.17) \times 10^3$ sec^{-1}.

I. INTRODUCTION

UNTIL recently, the only accurate data concerning the interaction between the muon and the atomic nucleus were obtained from total-capture-rate measurements with complex nuclei.[1,2] The inherent difficulty of the attempt to extract the basic form of the muon-nucleon weak coupling then naturally suggested exploring the possibility of observing muon capture by protons and other light nuclei, such as deuteron and He^3, where an understanding of the nuclear structure may be more accessible.

Recently, measurements of the muon-capture rate in $(p\mu p)^+$ molecular ions were carried out independently by using hydrogen-bubble-chamber[3] and scintillation-counter techniques[4]; and the rate of the μ-He^3 reaction into neutrino and H^3 has since been obtained with rather good accuracies[5] (i.e., of the order of a few percent). Although the hydrogen results are statistically limited and there are still some uncertainties in the detailed nuclear structure of He^3 and H^3, the experimental results can be said to agree remarkably well with the theory. But even with the accuracy of the He^3 measurements, the rather intricate, theoretically predicted pion-induced coupling effects in muon capture are only crudely tested, simply because the He^3 rate is not very

* Work supported in part by U. S. Office of Naval Research under contract No. ONR-266 (72).

† Submitted in partial fulfillment of the requirements for the degree of Doctor of Philosophy in the Faculty of Pure Science, Columbia University. Present address: Carnegie Institute of Technology, Pittsburgh, Pennsylvania.

‡ Present address: Brookhaven National Laboratory, Upton, New York.

§ Present address: Rutgers, The State University, New Brunswick, New Jersey.

‖ Present address: University of Rochester, Rochester, New York.

¶ Present address: Yale University, New Haven, Connecticut.

[1] J. C. Sens, Phys. Rev. **113**, 679 (1959); M. Eckhause, Carnegie Institute of Technology Report No. 9286, 1962 (unpublished); T. A. Filippas, P. Palit, R. T. Siegel, and R. E. Walsh, Carnegie Institute of Technology Report No. NYO 10563, 1963 (unpublished).

[2] A review of the present status of muon-capture physics can be found in the article: G. Feinberg and L. M. Lederman, Ann. Rev. Nucl. Sci. **13**, 431 (1963).

[3] R. H. Hildebrand, Phys. Rev. Letters **8**, 34 (1962).

[4] E. Bleser, L. Lederman, J. Rosen, J. Rothberg, and E. Zavattini, Phys. Rev. Letters **8**, 128 (1962); J. Rothberg, E. W. Anderson, E. J. Bleser, L. M. Lederman, S. L. Meyer, J. L. Rosen, and I-T. Wang, Phys. Rev. **132**, 2664 (1963).

[5] L. B. Auerbach, R. J. Esterling, R. E. Hill, D. A. Jenkins, J. T. Lach, and N. H. Lipman, Phys. Rev. Letters **11**, 23 (1963); I. V. Falomkin, A. I. Filippov, M. M. Kulyukin, B. Pontecorvo, U. A. Scherbakov, R. M. Sulyaev, V. M. Tsupko-Sitnikov, and O. A. Zaimidoroga, Phys. Letters **3**, 229 (1963); R. M. Edelstein, D. Clay, J. W. Keuffel, and R. L. Wagner, Jr., *Proceedings of the Conference on Fundamental Aspects of Weak Interactions* (Brookhaven National Laboratory, Upton, New York), 1963.

sensitive to these effects. The capture rate from the $(p\mu p)^+$ molecule has a more sensitive dependence on $g_P{}^\mu$. The most accurate measurement of the rate contains a 9% uncertainty. To extract information about the coupling constants, it was necessary to make some simplifying assumption. The most plausible one is the universality of conserved vector current (CVC), in view of the recent successful experimental verification[6,7] of the CVC theory[8] in both O^{16} β decay and π^+ β decay. As a result of analysis of the $p\mu p$ data, a possible region of variations of $g_P{}^\mu/g_A{}^\mu$ and $g_A{}^\mu/g_V{}^\beta$ was obtained.

In any case, it remains highly desirable to obtain information from other sources. Besides the rather interesting case of μ capture by O^{16},[9] a logical choice appears to be the μ-d capture process: $\mu^-+d\rightarrow\nu+2n$. It is in fact the last candidate in the very-light-nucleus category to be studied experimentally. The detection of μ-d capture has been delayed mainly by the following difficulties: (1) extremely low capture rate, (2) lack of an efficient device to detect neutrons in a broad range of energy, (3) complications from molecular and fusion processes in liquid hydrogen (or deuterium), and (4) demand of extremely high degree of purity of the liquid hydrogen (or deuterium). At the moment it appears that the major difficulty in observing the μ-d capture in pure liquid deuterium comes from the third category, i.e., the atomic and molecular complications. The available experimental results[10] indicate that the $(d\mu d)^+$ molecule formation rate is considerably higher than the theoretically predicted number.[11] It appears therefore that the idea of observing muon capture from the atomic states of μd in liquid deuterium could not be realized.

The attempt here is neither to pursue the idea just stated, nor to prove it false. We have merely tried a different approach. The observation of the μ-d capture process was carried out with a liquid-hydrogen target that contained only a small amount of deuterium. The recent study of muon capture in pure hydrogen[4] and the molecular and fusion processes in deuterated hydrogen[12] made it feasible to observe the μ-d capture process by way of the $(p\mu d)^+$ molecules formed in the liquid hydrogen with a very low deuterium concentration. Along with the $(p\mu d)^+$ formation, some complicated but interesting muon-capture processes take place as a result of the muon-catalyzed fusion of p-d into He^3. These are the breakup channels of muon capture by He^3 that can be detceted by neutron counters:

$$\mu+\mathrm{He}\rightarrow\nu+n+d$$
$$\rightarrow\nu+2n+p.$$

In this paper we wish to show how the μd capture rate and the μ-He^3 neutron rate are extracted from the observed time distribution of neutrons initiated by the various muon atomic and molecular systems.

In Sec. II we describe the main experimental techniques employed. Some of these techniques were used before in the experiments[4,12] on muon capture in pure hydrogen and on muon molecules in hydrogen recently reported. A brief study of the physics related to the $(p\mu d)^+$ molecular ion is given in Sec. III, with particular emphasis on the molecular-ion formation, hyperfine structure, and muon-nucleon overlap probabilities. Data analysis and discussion of the results are given respectively in Secs. IV and V.

II. EXPERIMENTAL PROCEDURES

A. Beam

A low-momentum muon beam of average energy 60 MeV was extracted from the Nevis synchrocyclotron through a magnetic field free channel. It was first bent through 41° by a wedge-shaped dipole magnet, and then focussed further by a pair of quadrupole magnets to a liquid-hydrogen target. The negative meson beam was normally composed of pions, muons, and electrons in the approximate ratios of 7:1:7. To obtain a highly purified muon beam it was necessary to make a careful momentum selection of the beam particles. This is important for the present experiment, because both pions and electrons would give rise to unwanted accidental backgrounds, and an excess of electrons in the beam would make it difficult to determine accurately the number of muons stopping in the target. The meson beam was first peaked in its total intensity; a further increase of the magnetic field intensity of the bending magnet then enabled us to select a beam of higher momentum and hence relatively more muons. In this manner it was possible to achieve a purity level of the muon beam close to 99% while losing only half the muons. The beam profile was carefully checked both by repeated runs of range curves, and by a time-of-flight device. Since the beam compositions and the shielding arrangements are very similar to those used before in the $(p\mu p)^+$ experiment,[4] we shall avoid repeating the detailed figures and description here.

[6] Y. K. Lee, L. Mo, and C. S. Wu, Phys. Rev. Letters **10**, 253 (1963).

[7] P. Depommier, J. Heintz, C. Rubbia, and V. Soergel, Phys. Letters **5**, 61 (1963); D. Bartlett, S. Devons, S. L. Meyer, and J. Rosen, Phys. Rev. **136**, B1452 (1964).

[8] R. P. Feynman and M. Gell-Mann, Phys. Rev. **109**, 193 (1958); S. Gershtein and Ya. B. Zel'dovich, Zh. Eksperim. i Teor. Fiz. **29**, 698 (1955) [English transl.: Soviet Phys.—JETP **2**, 576 (1957)].

[9] R. Cohen, S. Devons, and A. Kanaris, Nucl. Phys. **57**, 255 (1964); A. Astbury, L. B. Auerbach, D. Cutts, R. J. Esterling, D. A. Jenkins, N. H. Lipman, and R. E. Shafer, Nuovo Cimento **33**, 1020 (1964).

[10] J. D. Fetkovich, T. H. Fields, G. B. Yodh, and M. Derrick, Phys. Rev. Letters **4**, 570 (1960); J. H. Doede, Phys. Rev. **132**, 1782 (1963).

[11] S. Cohen, D. L. Judd, and R. J. Riddell, Jr., Phys. Rev. **119**, 397 (1960); Ya. B. Zel'dovich and S. S. Gershtein, Usp. Fiz. Nauk **71**, 593 (1960) [English transl.: Soviet Phys.—Usp. **3**, 593 (1961)].

[12] E. Blesser, E. W. Anderson, L. M. Lederman, S. L. Meyer, J. L. Rosen, J. Rothberg, and I-T. Wang, Phys. Rev. **132**, 2679 (1963); see also G. Conforto, S. Focardi, C. Rubbia, and E. Zavattini, Phys. Rev. Letters **9**, 432 (1962) and **9**, (E)525 (1962).

B. Target

The construction of the target is dictated mainly by the following two requirements:

(1) The target wall, besides being adaptable to a wide range of temperatures and pressures, should be composed of exclusively high-Z elements (muon-capture rate $\propto Z_{\text{eff}}^4$), and should be arranged in such a manner that the beam particles would have as little chance to interact with it as possible.

(2) A very high degree of purity of the liquid hydrogen is demanded because of the possibility of transfer of muons from hydrogen isotopes to the relatively high-Z impurities dissolved in the liquid hydrogen. The transfer rate is generally close to 10^{11} sec^{-1}.

The first requirement is clearly necessary in making a time separation of the wall events from the muon-capture events of interest. This was met by constructing the target wall of 0.025 in. of stainless steel with silver lining, and using a thin beam window (0.01 in. of stainless steel). The radiation shield is made of thin silver foil.

To achieve a high degree of purity of the liquid hydrogen we used a commercial palladium hydrogen purifier in the input. Palladium allows only hydrogen isotopes to diffuse through, and discriminates totally against other gases (for example, He, O_2, and N_2, etc.). Further precautions were taken in welding the target wall in oxygen-free and flux-free conditions, and in baking it for several days before running the experiment so as to ensure a minimum of outgassing of impurities from the wall during the experiment. We have examined carefully three possible sources of impurities: (1) the residual gas in the target after evacuation; (2) impurities infiltrating the heated palladium coil; (3) outgassing from the target walls during the run and minor leaks. The evacuation of the pure system was done with a titanium getter pump and a cryogenic pump so as to avoid possible contamination by carbon compounds from the conventional oil pumps. The final pressure reached after the evacuation and baking processes was approximately 6×10^{-7} mm of Hg at liquid-nitrogen temperature ($\sim$77°K). The leak-up rate through the palladium was checked for both helium and nitrogen gases. The rate measured in the vacuum on the output side of the purifier remained constant, regardless of whether the input side is a vacuum, or 100 psi of helium or of nitrogen. Therefore, the impurities due to the first two sources were as low as 10^{-11}. The constancy of the muon-capture rate measured over the several weeks of running is a clear evidence that the third source of impurities is completely negligible.

The isotopically pure liquid hydrogen used in a previous experiment[4] on muon capture by the $(p\mu p)^+$ molecular ion was used again in this experiment by adding 0.32% of deuterium. A relatively minor portion of the experiment was done with 515-ppm deuterium concentration. The deuterium-adding process involved first an increase of pressure of the pure hydrogen to about 10 psi and then the dumping of 10 cu ft at STP to an adjoining vacuum tank. A measured amount of deuterium was then introduced to the pure system via the palladium followed by flushing with 10 cu ft of the pure hydrogen gas.

C. Scintillation Counters and Logic

1. Beam and Electron Counters

The arrangement of the beam telescope as described in Fig. 1 is rather conventional, except that counter Nos. 1 and 3b are made of very thin plastic scintillators. Clearly, thin counters help to diminish scattering of the beam, and in particular No. 3b was chosen to be extremely thin (0.02 in.) to prevent possible muon capture by low-Z elements in the plastic. The combination of counters Nos. 3a and 3b (Fig. 1) helped to eliminate unwanted accidental coincidences, for example, due to a muon stopping in the beryllium moderator and a noise pulse in counter No. 3b.

The electron counters labeled A_1, A_2, A_3, and A_4 are made of $11\frac{1}{2}\times14\times\frac{3}{8}$ in. plastic scintillator wrapped in black Mylar, and are arranged to surround the hydrogen target in the manner of a rectangular box. They are used in defining the number of muon stoppings, designated as $\mu\text{-stop}\equiv(1)(2)(3a)(3b)\Sigma_i\bar{A}_i$; and in coincidence with the neutron counters (N_i) they serve to count the decay electrons: $e\equiv(\sum_i N_i)(\sum_i A_i)$.

The μ-stop pulse in turn initiates two 7-μsec-long gates: the "real" gate (delayed for 0.7 μsec relative to the muon pulse), and the "accidental" gate (delayed for 13 μsec relative to the muon pulse). The electron pulse sent through the "real" gate defines a "real" electron e_r and that through the "accidental" gate e_a.

2. Neutron Counters and n-γ Discrimination

In the experiment we used three $4\times5\times6$ in. glass boxes each containing the liquid scintillator NE213. A NaI crystal on the fourth side of the target was used to detect the fusion gamma rays. The neutron counters were carefully filled in sealed nitrogen gas chambers and de-oxygenated by further nitrogen flushing before the run and were packed with magnesium oxide powder on the outside to optimize light collection. These were viewed by 9530B EMI photomultipliers from the 5-×6-in. faces. The Brooks technique that makes use of the saturation effect of the fast component of the recoil-proton scintillation was already described in great detail in connection with the $(p\mu p)^+$ experiment.[13] In this experiment, as in the previous one, we verified the γ rejection efficiency by continuous monitoring of the n-γ "gap" in the pulse-height-versus-tail display.

---

[13] J. E. Rothberg, Columbia University Nevis Report No. 116, 1963 (unpublished).

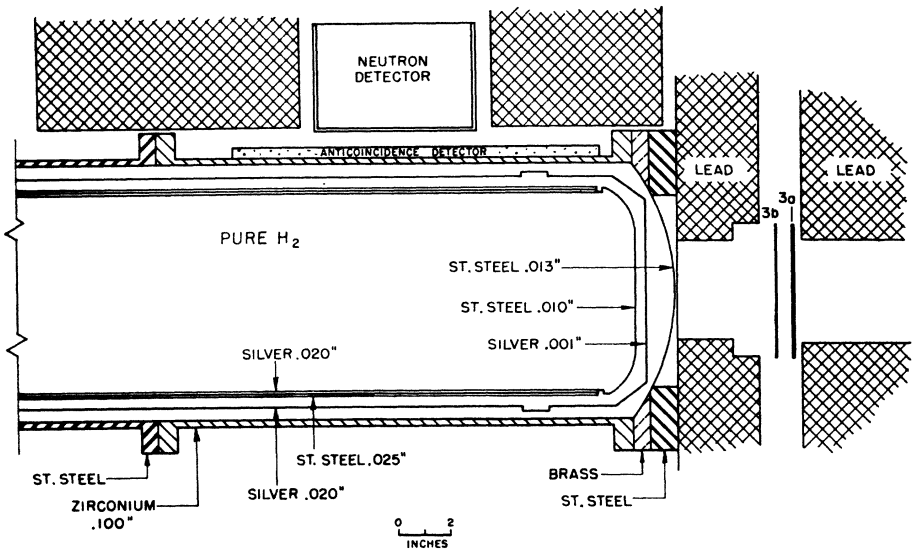

FIG. 1. Diagram showing the beam telescope and the liquid-hydrogen target with the arrangement of the local shielding, and the electron and neutron detectors.

3. Logic for "Pion" and "Electron" Events

A pulse from beam counter No. 1 was displayed on the fast trace (Tektronix 517 oscilloscope) and used for an effective $(\sum_i N_i)$ $\bar{1}$ to remove prompt neutron events from pions in the beam. Similarly, a branch of the mixed output of the electron counters $\sum_i A_i$ was used to discriminate against neutron events accidentally recorded with a muon that decayed into an electron. This was shown on the Tektronix 555 oscilloscope.

III. THE $(p\mu d)^+$ MOLECULAR ION

A. Formation and Hyperfine Effects of the $(p\mu d)^+$ Molecular Ion

As the level of deuterium concentration is raised, more and more muons are transferred from protons to deuterons; and when it gets close to 1%, practically all the stopped muons are transferred to deuterons in less than 10^{-7} sec. The μd atom will then collide with a proton in their mutual S state to form a $(p\mu d)^+$ molecular ion. During this process the orbital electron is ejected, and the $p\mu d$ three-body system undergoes an electric-dipole transition from the continuum S state to the $L=1$ rotational state.[10] The positively charged ion immediately picks up another orbital electron (in approximately 10^{-11} sec) and forms a neutral system. This neutral system is, however, highly unstable, and will relax into its $L=0$ ground state at a rate of $\sim 10^{11}$ per sec (Fig. 2). The presence of the electron is essential to this rapid transition, which is again an electric-dipole emission. Consequently, in the muon-capture problem one has only to deal with the ground state of the $(p\mu d)^+$ system, unlike the case of $(p\mu p)^+$ molecular ion in pure liquid hydrogen where the overwhelming mode of muon capture takes place in the metastable $L=1$ ortho state. It is important to realize that there exist several distinct hyperfine states of the $(p\mu d)^+$ molecular ion, because the muon-capture rates from these states are widely different. The spin configurations in the $(p\mu d)^+$ ions can be obtained in the following manner. It is known that at sufficiently low deuterium concentration (<1% say) the μd atomic spin states are statistically populated. This is a consequence of the low depolarization rate of muons in the exchange collision of μd with another d, as indicated by both theoretical[14] and experimental[12] results. It is expected to be roughly 10^3 times smaller than the rate of μ depolarization by μp exchange collision with another proton. In this experiment the liquid hydrogen is deuterated to 0.32%. Therefore, it is quite safe to assume that the μd atoms all have statistical spin populations to start with. It follows that the resulting $(p\mu d)^+$ systems also have

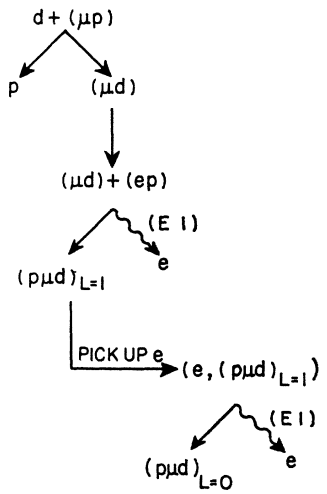

FIG. 2. Schematic diagram of the formation of the ground state of $(p\mu d)^+$. Shown are the various molecular processes leading from the initial stage of μp atom to the final stage of $L=0$ state of $(p\mu d)^+$.

[14] S. S. Gershtein, Zh. Eksperim. i Teor. Fiz. **40**, 698 (1961) [English transl.: Soviet Phys.—JETP **13**, 488 (1961)].

purely statistical spin populations, since the transitions leading from μd to the final $L=0$ configuration of the $(p\mu d)^+$ ion, as we noted before, are merely electric-dipole transitions which do not affect the effective spin populations.

There are in total four hyperfine states of the $(p\mu d)^+$ molecular ion, corresponding to $J=2$, $J=1$, (two levels), and $J=0$. Since the magnetic coupling between the two nuclear particles is negligible compared to their spin interactions with the muon, the effective interaction Hamiltonian h can be written as

$$h=g_p(\mathbf{S}_\mu\cdot\mathbf{S}_p)\langle r_{\mu p}^{-3}\rangle+g_d(\mathbf{S}_\mu\cdot\mathbf{S}_d)\langle r_{\mu p}^{-3}\rangle,$$

with $g_p\cong 2.79$ and $g_d\cong 0.86$. It is a straightforward problem to solve for the eigenfunctions and the energy values associated with the various hyperfine states. Such solutions have been obtained independently by Gershtein and Zel'dovich and by Cohen, Judd, and Riddell, mainly to study the pd fusion problem.[10]

B. Muon-Catalyzed Fusion and the Measurement of Molecular Constants

Historically, the earliest interest in the $(p\mu d)^+$ molecular ion was found in its relation with the muon catalysis of the pd fusion process[15]:

$$p+d\rightarrow \mathrm{He}^3+\gamma(5.5\ \mathrm{MeV}).$$

The reaction rate of this process was found to be strongly spin-dependent. A detailed theoretical study[10] revealed that the predominant mode of fusion is that of a magnetic-dipole transition from the total nuclear spin $S=\frac{1}{2}$ state. On the basis of this assumption and the spin configurations of the $(p\mu d)^+$ ion arrived at in Sec. III A, a set of rather accurate determinations of the molecular constants and the fusion rate was carried out. Of particular interest are the $(p\mu d)^+$ formation rate λ_{pd} and the pd fusion rate λ_f. These were found by a least-squares fitting of the 5.5-MeV gamma-ray yield versus time at 0.32 and 0.72% deuterium concentrations to be[12]

$$\lambda_{pd}=(5.80\pm 0.30)\times 10^6\ \mathrm{sec}^{-1},$$
$$\lambda_f=(0.305\pm 0.010)\times 10^6\ \mathrm{sec}^{-1}.$$

As is well known, the fusion rate λ_f is divisible into two parts $\lambda_f=\lambda_1+\lambda_2$, λ_1 for the process with a 5.5-MeV gamma-ray emission ($M1$ transition), and λ_2 for fusion with emission of a muon by internal conversion ($E0$ transition). They were measured to be[12]

$$\lambda_1=(0.256\pm 0.012)\times 10^6\ \mathrm{sec}^{-1},$$
$$\lambda_2=(0.049\pm 0.010)\times 10^6\ \mathrm{sec}^{-1}.$$

In the following, we will use the various constants to deduce the populations, as a function of time, of the various hyperfine states in the $(p\mu d)^+$ molecular ion. They are found, as expected, to depend mostly on simple linear combinations of λ_f and λ_0 (μ decay rate) which are quite accurately known. Therefore, the uncertainties involved in the knowledge of the populations are only of the order of a few percent.

[15] L. W. Alvarez, H. Bradner, F. S. Crawford, Jr., J. A. Crawford, P. Falk-Variant, M. L. Good, J. D. Gow, A. H. Rosenfeld, F. Solmitz, M. C. Stevenson, H. K. Ticho, and R. D. Tripp, Phys. Rev. **105**, 1127 (1957).

C. Hyperfine Populations

The time distributions of the formed μ-He^3 atom and the four separate levels of $(p\mu d)^+$ hyperfine states can be deduced in a straightforward manner by solving numerically the set of linked parent-daughter type of first-order linear differential equations. But to extract the muon-capture rates, it is more expedient to work in terms of the μp and μd hyperfine states. Let us, therefore, write down the simple relations between the effective μp, μd hyperfine populations and the various $(p\mu d)^+$ hyperfine populations. Suppose we denote the total wave function of the $(p\mu d)^+$ system in the hyperfine state J by Ψ_J. We will choose two of the particles μ and d, and denote their total spin by J'. Then Ψ_J can be written as a linear combination of $\Psi_{JJ'}$ which are the simultaneous eigenfunctions of J^2, J_Z, and J'^2. Thus,

$$\Psi_J=\sum_{J'} C_{JJ'}\Psi_{JJ'}.$$

From the above relation one can easily obtain the relation between the two sets of hyperfine populations:

$$N_{J'}(t)=\sum_J (C_{JJ'})^2 N_J(t),$$

where $N_J(t)$ denotes the total population in the hyperfine state J. The numerical values of $C_{JJ'}$ are given in Table I for different choices of particle pairing in J'. The results for the μ-He^3, μp-singlet, and μd-doublet populations for a single starting μ are plotted in Fig. 3. They form the basis of the separation of μd and μ-He^3 events from the μp events. It is interesting to note that the μp singlet population (characteristic time $\cong 1.48$ μsec) is significantly lower than the μd doublet population (characteristic time $\cong 1.65$ μsec). With a further depreciation in the muon density at the proton relative to that at the deuteron (approximately a factor 0.65), the fraction of muon-capture events attributed to the μp mode is not as high as might have been expected.

TABLE I. $C_{JJ'}$.

	$\mu+p$		$\mu+d$		$p+d$	
J	$J'=0$	$J'=1$	$J'=\frac{1}{2}$	$J'=\frac{3}{2}$	$J'=\frac{1}{2}$	$J'=\frac{3}{2}$
2	0	1.0	0	1.0	0	1.0
1 (upper)	0.235	0.97	0.655	0.754	0.93	0.37
1 (lower)	−0.97	0.235	−0.754	0.655	−0.37	0.93
0	0	1.0	1.0	0	1.0	0

D. Muon Densities

We have obtained the muon densities at the proton γ_p and at the deuteron γ_d, using the wave functions obtained by Cohen, Judd, and Riddell (CJR).[10,16] These are the values of $|\Psi(\mathbf{r}_\mu,\mathbf{r})|^2$ averaged over the nuclear coordinates $\mathbf{r}\equiv\mathbf{r}_d-\mathbf{r}_p$. The actual numerical integration was carried out on the IBM-1620 computer at Nevis Laboratory. The results are

$$\gamma_p=0.589(\pi a_p^3)^{-1},$$
$$\gamma_d=0.770(\pi a_d^3)^{-1},$$

where a_p and a_d are the Bohr radii for the μp and μd atoms, respectively. The nuclear wave functions obtained in the CJR formulation[10] resemble very closely the well-known Morse type of wave functions except for small internuclear distances. The muon wave functions are variational wave functions[16] that satisfy correct asymptotic conditions for both zero and infinite internuclear distances.

IV. DATA ANALYSIS

A. Collection of Raw Data

In Sec. II we have defined the "μ-stop" pulse and the μ-gated "real neutron" pulse. The latter pulse had a rather wide range of amplitudes. Therefore, it was branched out into two signals, and one of them was attenuated by a factor 4 relative to the other. The "time" of the muon-capture event was simply given by the relative distance-between the μ-stop pulse and the attenuated neutron-amplitude pulse measured on film. The latter was used as the triggering pulse of the Tektronix 555 oscilloscope. Films collected during the 0.32% deuterium concentration" run and the "515 ppm deuterium concentration" run provided the main body of the raw data. The entire group of raw data used in our analysis covered a time interval from 0.8 to 8.0 μsec.

Among all the pictures scanned, only about 60% were accepted as possible candidates for muon-capture neutrons. They were selected on the basis of the following criteria:

(1) presence of a single "neutron-amplitude" pulse, and the associated "neutron-tail" pulse;
(2) presence of the "μ-stop" pulse ("real" or "accidental");
(3) absence of the "electron" pulse;
(4) absence of the "pion" pulse.

These candidates were further screened through the n-γ discrimination process. This was done by plotting the measured height of the "neutron-tail" pulse versus the height of the "neutron-amplitude" pulse, and comparing with some separate tail-versus-amplitude plots of Pu-Be source pictures and γ-ray source pictures. After the n-γ screening process, the final qualification for the neutron candidates was that the neutron pulse amplitude has to be larger than a fixed number determined from the γ-ray source data. The actual lower limit corresponded to 0.9-MeV γ ray.

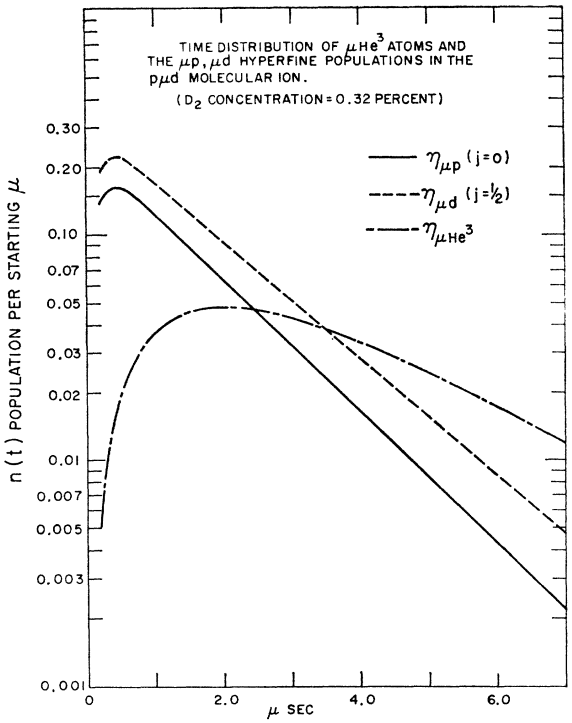

FIG. 3. Distributions in time of the effective singlet state of μp, doublet state of μd in the $(p\mu d)^+$ molecules and of the μ-He^3 atoms formed in the liquid hydrogen with 0.32% deuterium concentration.

Events that satisfy all the above-mentioned conditions are considered as "qualified" muon-capture events. A small fraction of these corresponds to accidental neutrons; these were distinguished from the real events by the presence of the "accidental μ" pulse. The qualified real events were then grouped into 14 time channels (Fig. 4), with a channel width of 0.505 μsec. On the basis of linearity of the scope and a time measurement somewhat finer than 0.04 μsec, the resolution was certainly better than 10% of the channel width.

The entire run of the experiment described here covered a period of 17 days. The actual data collection took about 110 h. The rest of the time was spent mainly in beam checks and in making various calibrations of the neutron-detecting apparatus. This group corresponds to approximately 1.25×10^8 muons stopping in the liquid-hydrogen target.

The neutron rate was found to be practically constant during the entire run, a result that reassured us regarding the purity of the liquid hydrogen. In addition

[16] S. Cohen, D. L. Judd, and R. J. Riddell, Jr., University of California Radiation Laboratory Report No. UCRL-8802, 1959 (unpublished).

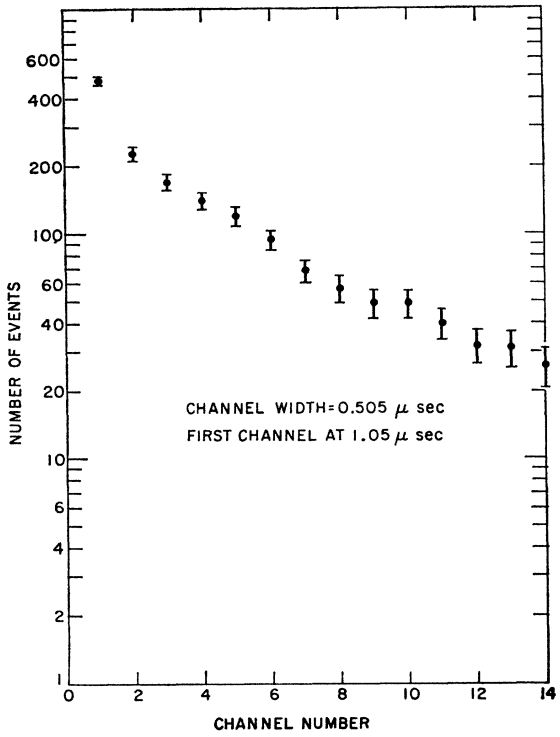

FIG. 4. Time distribution of the raw neutron events observed.

to all the precautions taken during the experiment, a thorough check was made of the internal consistency of the data with respect to time distribution, background subtraction, and energy scales, etc.

B. Background Events

1. Wall Events

In the experiment of muon capture in pure hydrogen,[4] reported previously, the "real" gate was started at 0.5 μsec, and the geometry and muon beam used were identical to ours for a major portion of that experiment. Therefore it was a very useful source of information about the rate of wall capture in the present experiment. Since the knowledge of "time" of the capture event played a much more critical role in this experiment than in the previous one, we took care in re-examining the time measurements of all the early events recorded in the $p\mu p$ experiment. A rather trivial curve fitting was carried out (separately for each of the neutron counters) for the early events after subtracting the extrapolated 2.2-μsec "background" attributed to muon-capture neutrons. The characteristic time was found to be approximately 0.2 μsec corresponding to muon captures in iron.

2. Photoneutron Events

Photoneutrons caused by decay-electron bremsstrahlung formed the major source of our background subtraction. The rate of these events was measured by stopping positive muons in the liquid-hydrogen target. Roughly 100 to 150 events for each neutron counter were recorded. These events, after multiplication by the proper (e_r-e_a) and gate ratios, were assumed to have a characteristic time of 2.2 μsec.

3. $p\mu p$ Events

At 0.32% deuterium concentration, this group of capture events formed the least significant correction to the raw data. However, the 515-ppm deuterium-concentration data contained a rather significant amount of $p\mu p$ events ($\sim$10–15%). To account for this correction properly, we solved numerically the differential equation

$$dN_{p\mu p}/dt=\lambda_{pp}N_{\mu p}-\lambda_0 N_{p\mu p}.$$

(The dependence on deuterium concentration is contained in $N_{\mu p}$.) as one of the coupled differential equations. The background could thus be obtained by normalizing the $p\mu p$ data to the proper (e_r-e_a) number, and it was assumed to have a functional form $N=N_0e^{-t/2.2}$ after a very short time interval characteristic of the $\mu p+d\rightarrow\mu d+p$ process. N_0 was then determined by comparison with the actual numerical solution.

4. Accidentals

During the run a 7-μsec delayed gate (from 13 to 20.3 μsec) was used to measure the flat background of accidentals. The entire raw data that satisfied the condition of neutron-pulse amplitude (the lower limit was set at 0.9-MeV gamma-ray scale) involved $\lesssim$10% ($\sim$150) accidentals.

5. π^- and e^- Accidentals

The π^- and e^- pulses on film which were used for the rejection of events had a small number of accidentals included among them. The origin of time of the π^- pulse was determined from the sharp peak of the scanned π^- time distribution. A small number of π^- events before zero time in an interval $\sim$0.15 μsec was obtained. Extended to the entire gate it amounted to roughly one-quarter of the accidentals in Sec. IVB4. Similarly, we obtained an e^- accidental rate of the order of one-sixth of the accidentals in Sec. IVB4. Clearly, such corrections had the effect of increasing slightly the event rate.

6. μp Capture Events

Assuming the knowledge of spin configurations of the $(p\mu p)^+$ and $(p\mu d)^+$ molecular ions, one can easily sort out the portion of expected μp events in the $(p\mu d)^+$ data. This was done by subjecting the relevant part of $(p\mu p)^+$ data to the same amplitude and gate conditions as used throughout the present analysis. While the theoretical result for the muon-proton overlap ratio between $(p\mu p)^+(2\gamma_0=1.165)$ and $(p\mu d)^+(\gamma_p=0.589)$ is

assumed, the uncertainties in the number of muon stoppings and the neutron counter efficiency are clearly not involved in this subtraction.

C. Curve Fitting

Once the various background events are properly assessed, the resulting neutron events can be attributed entirely to muon captures by deuterons and He^3 (Table II). The "corrected" time distribution of neutrons is plotted in Fig. 5. A very minor portion of it (approximately 22 events) is expected to come from muon capture in the quartet ($j=\frac{3}{2}$) hyperfine state of μd. As in the case of μp capture, we assume that the ratio between the rates of muon capture in the two separate μd hyperfine states is known.[17] There should be no danger in making this assertion, because not only is the ratio itself very small, but also it is not significantly affected as the relatively unknown factor, e.g., the value of $g_P{}^\mu/g_A{}^\mu$, is varied.

To extract the muon-capture rates a two-parameter curve fitting of the corrected neutron time distribution was made. Suppose the number of neutrons in the ith time channel t_i is denoted by N_i, with an uncertainty ΔN_i. The two unknown parameters λ_1 and λ_2 in the distribution

$$f(t_i)=\lambda_1 f_1(t_i)+\lambda_2 f_2(t_i)$$

take the most probable values for the given data when the χ^2 value is minimum.

In the standard treatment of least squares, the mean-square deviation of the parameter Λ_α is given by the α diagonal matrix element of the inverse of the C matrix. This is based on the assumption that the measurements at two different channels are statistically independent. This is clearly not true in our case where a fairly large portion of smooth hypothetical background has been subtracted. The background in the ith channel is correlated to that in the jth channel in the sense that the knowledge of one is not independent of the knowledge of the other. To take care of this effect one estimates the mean square deviation between the least-squares valuation of the parameter Λ_α and its true value $\Lambda_{\alpha 0}$. Such treatment can be found, for example, in the paper of Rose.[18]

$$\langle(\Lambda_\alpha-\Lambda_{\alpha 0})^2\rangle=[(\textstyle\sum_i\langle v_i{}^2\rangle)/(m-l)]C_{\alpha\alpha}{}^{-1}$$
$$\cong[\chi^2/(m-l)]C_{\alpha\alpha}{}^{-1}.$$

In the above, the expression $\langle v_i{}^2\rangle$ implies that the averaging process should in principle be carried out over a large number of experiments [m=channel number, and l=number of parameters].

Figure 5 shows the fitted curves of $\lambda_1 f_1$, $\lambda_2 f_2$, and f; we obtain $\chi^2\cong 5.0$. In the following, we will try to relate λ_1 and λ_2 to the μd capture rate and the μ-He^3 neutron rate, using the known results (Sec. III) of μd and μ-He^3 populations represented by $f_1(t)$ and $f_2(t)$.

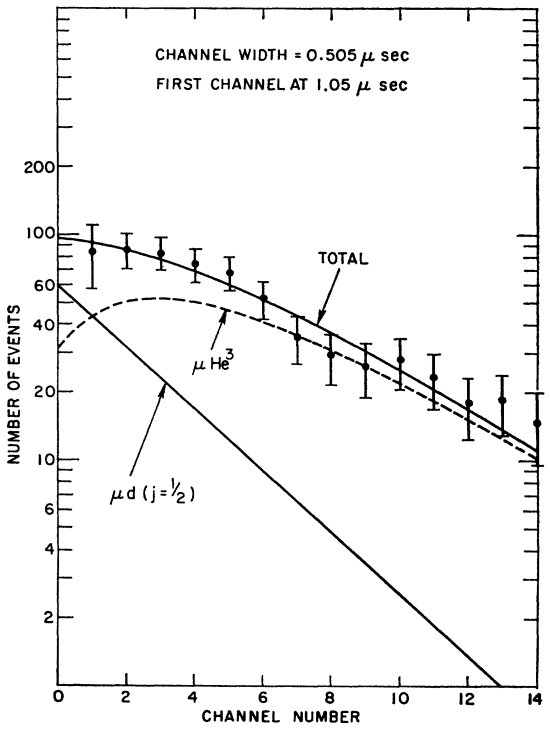

FIG. 5. Time distribution of the corrected neutron events that are attributed to muon capture by deuteron and by He^3.

TABLE II. Composition of observed neutron events. Time interval: 0.8–8.0 μsec. Energy interval: $E>0.9$ MeV (gamma-ray scale).

Wall events	301±54
Photo-neutron events	329±20
$p\mu p$ events	62±4
"μp" events	185±11
Accidentals	156±13
π^- accidentals	35±8
e^- accidentals	25±5
Corrected events	615±61

D. Muons Stopping in Hydrogen

Of all the beam particles counted as

$$(1)(2)(3a)(3b)\textstyle\sum_i \bar{A}_i,$$

a relatively small but nevertheless significant number corresponds to muons stopping in the front and side target walls, and in the 4-in. collimator rim immediately before the target. Therefore, to evaluate the number of muons that actually stop in the liquid hydrogen, we use the recorded number of decay electrons $e=e_r-e_a$. As we noted in Sec. II, the decay electrons were indicated by the coincidence of the

[17] I-T. Wang, this issue, Phys. Rev. **139**, B1539 (1965).

[18] M. E. Rose, Phys. Rev. **91**, 610 (1953).

neutron counters N_i with the electron counters A_i, and so they had approximately the same solid angle as the neutrons. Furthermore, they were subjected to the same delayed time gates as the neutrons (0.7-μsec delay for the real gate, and 13-μsec delay for the accidental gate), and they would come later than the charged particles produced by muons stopping in the high-Z target walls. As a consequence, the value of (e_r-e_a) was a very good measurement of the effective number of muons stopping in the liquid hydrogen. (The pure liquid hydrogen in the target extended over a distance of 23 in. along the beam direction. The average initial energy of the muons in the hydrogen was approximately 24 MeV. It was therefore quite safe to assume that the muons would not penetrate the entire length of the target.) The only non-negligible correction to this number comes from the decay electrons lost in the side walls of the target and other materials before the liquid scintillator. Let us call the total electron loss factor L. The number of muons stopping in liquid hydrogen is then given by

$$M=(e_r-e_a)/T\Omega L, \tag{1}$$

with T=time gate factor, Ω=electron solid angle.

The evaluation of Ω was done as part of a Monte Carlo program. It was found to be $\Omega=0.140\pm0.003$. The loss of electrons due to the target side walls was measured with a dummy target (composed of alternating layers of styrofoam and polystyrene) and layers of metals (average $Z=40$) simulating the target side walls. The $(e_r-e_a)/\mu$-stop ratios measured with the target walls in position and with them removed, indicated a 5% effect. The electron loss factor L, in the region between the target wall and the scintillator, and due to the energy threshold for counting electrons, was estimated to be 0.90 ± 0.05.

E. Neutron Counter Efficiency

The same Monte Carlo method used in the analysis of the $p\mu p$ data is applied to the evaluation of neutron counter efficiencies corresponding to neutrons from μd capture and from μ-He^3 capture. Unlike the case of μp capture that yields monoenergetic neutrons of 5.2 MeV, we have continuous neutron energy spectra typical of processes with three or more particles in the final channels. Therefore, the previous Monte Carlo program is extended to cover an energy range from 1.5 to about 20 MeV. A description of the program and a measurement of the proton response in scintillator NE213 was already reported in connection with the experiment on μ-capture in pure hydrogen.[13] In the following we will simply outline a few relevant points and the more important aspects of this method.

A substantial amount of information, or input data, about the actual experimental conditions is necessary in the program, in order to predict correctly the collective behavior of the neutrons initiated in the liquid hydrogen. It involves: (1) an accurate geometry of the target and the shielding arrangement surrounding it; (2) values of neutron scattering cross sections for all the relevant elements; (3) spatial distribution of muons stopping in the liquid hydrogen; (4) a given number of initial neutron histories (the number must be large enough to provide a statistical reliability of better than 5%); (5) pulse-height response of scintillator NE213 that relates proton and electron energies; (6) a given energy resolution of the neutron counter. The pulse-height response was taken to be

$$R=0.28E+0.033E^2, \quad E<6 \text{ MeV}$$
$$R=0.70E-1.330, \quad E>6 \text{ MeV}.$$

The nonlinear behavior occurs mainly in the low-energy region.

It is due to the ionized "column" created by the heavily ionizing particle along its path, which leads to the quenching of the light output, and the possible multiple scattering of low-energy neutrons in the scintillator. The measured results indicate that above 6 MeV the response becomes linear. We were not able to make any measurement above the neutron response of 9 MeV. However, since both the "saturation" effect and the double scattering of neutrons are expected to diminish at high energies, it seems perfectly safe to assume a linear behavior for the response throughout the high-energy region.

With the aforementioned input information, the Monte Carlo program was then able to take into account the various complications expected to happen to the muon-capture neutrons, such as scattering in the liquid hydrogen, the target walls, the lead shieldings, and the multiple scattering in the neutron scintillation counter. The output of the program is the pulse-height distribution of detected neutrons which can be used directly to evaluate the detector efficiency.

The program was run on the Columbia IBM-7094 computer. In each run a large number of histories of monoenergetic neutrons were followed. In the low-energy region ($E<3$ MeV), this number was taken to be 50 000 at $E=1.7$, 2, and 2.5 MeV. For $E\geq3$ MeV, it was run in steps of $\frac{1}{2}$ MeV, from 3 to 9 MeV, with 30 000 neutron histories each. From 9 to 20 MeV, it was only necessary to run the program in steps of 2 MeV, since the pulse-height distribution, as expected, becomes prefectly flat in the high-energy region. In our analysis we have used a pulse amplitude cut at 0.9 MeV (γ-ray energy). The distribution of pulse height was then integrated from this value up.

V. RESULTS AND DISCUSSION

We have seen that an important part of our data analysis has been the proper assessment of the origins of the detected neutrons. Results obtained from the background analysis are tabulated in Table II. The final distribution of the corrected neutron events was

TABLE III. Determination of muon stoppings.

C	$e(10^6)$	T	Ω	L	$M(10^6)$
0.32%	8.60	0.689	0.140	0.90	99.0
515 ppm	2.48	0.750	0.140	0.90	26.3
Uncertainty	~0	±1%	±2%	±5%	±5.5%

divided into two groups by the curve fitting program as indicated in Fig. 5. The knowledge of muon stoppings in hydrogen and neutron counter efficiency then serves to relate these results to the muon-capture rates of interest.

The curve fitting program described in Sec. IVC provides two useful numbers, i.e., the total number N_1 of neutrons from muon capture in the doublet state of μd, and the total number N_2 of μ-He^3 neutron events. The results are: $N_1=157\pm37.4$, $N_2=440.2\pm39.6$. The μd doublet capture rate R_1 and the μ-He^3 neutron rate R_2 can now be expressed in terms of N_1 and N_2, respectively, by the following relations:

$$R_\alpha=N_\alpha\left[Mf_\alpha\sum_{i=1}^{3}E_{\alpha i}\int_{0.8}^{8.0}n_\alpha(t)dt\right]^{-1},\quad \alpha=1,\,2. \quad (2)$$

In the above expression, M is the total number of muons stopping in the liquid hydrogen; f_α is the fraction of the energy spectrum observed; and $E_{\alpha i}$ is the product of the efficiency of the ith neutron counter with the fraction of its useful data-taking relative to the total number of muon stoppings. Starting with a single muon, $n_\alpha(t)$ is the probability at time t of the muon being in the α mode of the muonic systems as stated before in Sec. III (Fig. 3).

M is readily computed from Eq. (1). The numbers of stopping muons corresponding to the two different deuterium concentrations (0.32% and 515 ppm) are listed in Table III together with the data used to deduce them. Using the results from the Monte Carlo program we obtain ($E_\alpha\equiv\sum_{i=1}{}^3E_{\alpha i}$)

$$E_1=(1.99\pm0.16)\times10^{-2}\quad(\text{doublet }\mu d),$$
$$E_2=(1.49\pm0.12)\times10^{-2}\quad(\mu-\text{He}^3).$$

The above detector efficiencies have been obtained by averaging over the theoretical spectra obtained in the two following theoretical papers[17,19] from a minimum neutron energy of 1.4 MeV.

The numbers quoted are the net "efficiencies" of the entire neutron detecting system with respect to the total muon stoppings $M=(1.253\pm0.069)\times10^8$. The lower limit of neutron energy was determined from the relative efficiency curve and it gives $f_1=0.718$, $f_2=0.910$. Before presenting the final results for the capture rates, we wish to clarify a few points concerning

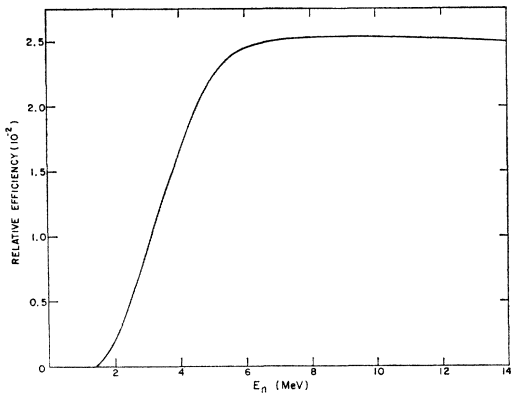

FIG. 6. Relative detector efficiency with respect to 30 000 starting neutron histories and a lower limit for pulse height corresponding to 0.9-MeV gamma-ray scale. It includes the solid-angle efficiency of the three neutron counters.

the evaluation of the neutron detector efficiencies. The fact that the average detector efficiencies depend on the energy distribution of the neutrons should in no way obscure our interpretation of the data. We see, from Fig. 6, that the relative efficiency for neutrons above 6.5 MeV is almost constant, and so the detector efficiency depends only on the relative effective spectrum amplitude in the 1.4- to 6.5-MeV region versus that in the region above 6.5 MeV. Qualitatively, it depends on the shape of the spectrum. As one can see, for example in the case of μd capture, the spectrum shape-affecting factors come about in the form of the final-state nuclear interaction and the neutrino and two-neutron kinematics. But within the range of uncertainty of the two-neutron singlet scattering length, the spectrum shape is only slightly influenced and the uncertainty in the efficiency is practically unchanged. Therefore, we believe that the efficiency estimate for the μd case is quite reliable. (The neutron counter efficiency E_1 given above has been derived from the neutron energy spectrum[17] based on a two-neutron singlet scattering length of -16.4 F. An earlier calculation[20] that employed the outdated value of -22 F gave an efficiency about 3.6% lower.) In the case of μ-He^3 the spectrum shape is less certain, and the comparison between the theory and the data is mainly used to test the consistency and the approximate magnitude of the neutron rate. We notice also that the detector efficiency for the μd process is larger than that for μ-He^3. This is mainly due to the presence of two neutrons in the final state of μd capture.

Finally, the "effective" time gate factors in Eq. (2) are given by $\int n_1dt=0.313\times10^{-6}$ sec, and $\int n_2dt=0.215\times10^{-6}$ sec with uncertainties of the order of 4%. Substituting the above results in Eq. (2), we obtain

[19] I-T. Wang, this issue, Phys. Rev. **139**, B1544 (1965).

[20] I-T. Wang, Columbia University Nevis Report No. 128, 1965 (unpublished).

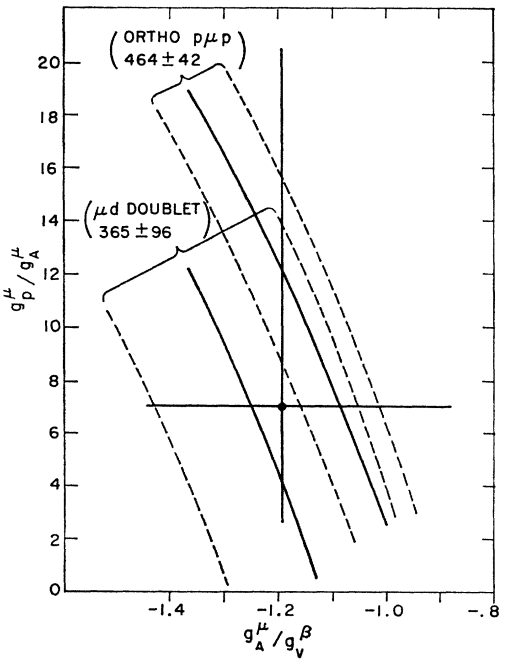

FIG. 7. Variations of $g_P{}^\mu/g_A{}^\mu$ and $g_A{}^\mu/g_V{}^\beta$ allowed by the measured rates of muon capture from the doublet state of μd and from ortho-$(p\mu p)^+$.

at once,

$$R_1 = 281 \pm 74 \text{ sec}^{-1}, \quad \text{(doublet } \mu d\text{)}$$

$$R_2 = (1.20 \pm 0.17) \times 10^3 \text{ sec}^{-1}, \quad (\mu - \text{He}^3).$$

The μ-d overlap factor obtained in Sec. IIID is $\gamma_d = 0.770(\pi a_d{}^3)^{-1}$. Therefore converted to the μd atom case the doublet μd capture rate becomes

$$R = 365 \pm 96 \text{ sec}^{-1}, \quad \text{(doublet } \mu d \text{ atom)}.$$

The theoretical number for this rate[17] is $R = 334$ sec^{-1}. In the following we will discuss the various implications of these measured rates.

VI. CONCLUSIONS

First of all we wish to point out that the result for the doublet state μd capture is a clear indication of the prominent Pauli exclusion principle effect. Using the most accurate measured ortho-$p\mu p$ capture rate[4] of 464 sec^{-1} and the muon-proton overlap factor[21] of $2\gamma_0 = 1.00$, one obtains a singlet μp capture rate of 614 sec^{-1}. If the μ-p overlap probability were the same as that of the μd atom, this number would become 718 sec^{-1}. The measured μd rate of 365 sec^{-1} is about half this number.

To apply the μd result to the unravelling of the induced coupling effects, we are somewhat handicapped by its uncertainty (26%). Nevertheless, it provides a region of variation of the coupling constants, which serves to restrict the possible values of $g_A{}^\mu$ and $g_P{}^\mu$. In Fig. 7 we have plotted the $g_P{}^\mu/g_A{}^\mu$ ratio against the $g_A{}^\mu$ and $g_V{}^\beta$ ratio as in the analysis of the $p\mu p$ data. We see that the predicted value of $g_P{}^\mu/g_A{}^\mu = 7.2$ and the $g_A{}^\beta/g_V{}^\beta$ ratio of -1.19 corresponds to a point well within the region allowed by the μd data. If we regard the region allowed by both the μd data and the $p\mu p$ data as being the "most favored" region, then it is possible to reduce significantly the uncertainties in the coupling constants.

In principle, if one could observe the low-energy neutrons (1 to 3 MeV) efficiently, one would measure a coupling constant combination significantly different from ours for the μd capture case. This is due to the sharp energy dependence of the I_s/I_t ratio[17] and would indeed be a very interesting and important thing to look into. In making the above analysis, we are of course fully aware of the possibility that the calculation of the muon-nucleon overlap factors could be somewhat off. But before a new and more reliable theory is developed for the $(p\mu d)^+$ system it seems pointless to make speculation here. In this respect, it is rather remarkable that a recent attempt[21] to study the $p\mu p$ molecular ion by an entirely different method than the one used by Cohen *et al.*[22] has yielded the value of 1.00 $(\pi a_\mu{}^3)^{-1}$ for the μp overlap probability in the $p\mu p$ ion. This seems to resolve the deviation between the measured and predicted ortho-$p\mu p$ capture rates.

The total muon-capture rate by He^3 is also of interest. Since the nuclear system is a composite of only three nucleons, it is still possible to compute the partial muon-capture rates to all the kinematically accessible final states without using the closure approximation. The muon-capture rates by He^3 to the $(\nu+n+d)$ channel (988 sec^{-1}) and the $(\nu+2n+p)$ channel (272 sec^{-1}) have been separately computed and are reported in a separate paper.[19] The combined predicted rate of these two modes is equivalent to a total neutron rate of 1.53×10^3 sec^{-1}. While it agrees quite well with some of the measured results by the Berkeley group[23] using low-pressure He^3 counters, it is significantly higher than their result of (700 ± 180) sec^{-1} obtained at higher pressures; but even here the deviation is not really violent since our measured neutron rate, converted to the net capture rate would amount to about 980 sec^{-1}, if the theoretical ratio for the two separate modes is assumed.

ACKNOWLEDGMENT

The authors are deeply indebted to Professor L. Wolfenstein for his clarifying comments and for reading an earlier version of the paper.

[21] W. R. Wessel and P. Phillipson, Phys. Rev. Letters **13**, 23 (1964); A. Halpern, *ibid.* **13**, 660 (1964).
[22] S. Cohen, D. L. Judd, and R. J. Riddell, Jr., Phys. Rev. **119**, 384 (1960).
[23] R. J. Esterling, University of California Radiation Laboratory Report No. 11004, 1964 (unpublished).